

Inhomogeneous tachyon condensation

Mark Hindmarsh and Huiquan Li
Department of Physics and Astronomy,
University of Sussex,
Brighton BN1 9QH,
U.K.

December 1, 2018

Abstract

We investigate the spacetime-dependent condensation of the tachyon in effective field theories. Previous work on Dirac-Born-Infeld effective action identified singularities in the field which appear in finite time: infinite gradients at the kinks, and caustics near local minima in the approximately homogeneous case, which are argued to represent the crossing of streams of non-interacting tachyon matter. By studying the solutions near stationary extrema and in linear perturbation theory, we show that caustics are not generic features of tachyon condensation. We also investigate the equation of state parameter of tachyon matter showing that it is small, but generically non-zero. This result, and the lack of caustics, calls into question the picture of tachyon matter as free-streaming particles. The linear analysis also shows that perturbations freeze in a short timescale, and that the classical field equations from the DBI and boundary string field theory effective actions become unstable at late time, with growth rates which diverge in the short wavelength limit. The energy density is shown to tend exponentially to zero near field maxima and infinity near field minima before the instability sets in. A proposal to regulate infinities by modifying the effective action is also studied. We find that although the infinities at the kinks are successfully regularised in the time-dependent case, the classical instability is still present. The presence of the instability indicates that the effective actions are both breaking down as the condensation proceeds.

1 Introduction

In Type II string theories, unstable branes of dimension p decaying into the stable ones with lower dimensions is well described by the Dirac-Born-Infeld (DBI) type

effective action [1, 2, 3]:

$$S = - \int d^{p+1}x V(T) \sqrt{1 + y}, \quad (1)$$

where $y = \eta^{\mu\nu} \partial_\mu T \partial_\nu T$, $V(T)$ is the asymptotic potential, and we use units in which $\alpha' = 1$. At the beginning of the condensation, the system has zero tachyon field $T = 0$ and is located on the top of the potential $V(T)$. It is unstable and will roll down when driven by a small perturbation. The field evolves towards the minimum of the potential $V = 0$, and the condensation ends. The final state corresponds to the disappearance of the unstable branes, replaced by “tachyon matter” whose properties are not well-understood.

The condensation process in the inhomogeneous case has also been studied. It has been realised that the equation of motion from the DBI action leads to solitonic solution with kinks and anti-kinks [4, 5, 6, 7]. At the kinks and anti-kinks, the field remains zero, and become daughter branes of one dimension lower at the end of the condensation. While the field in between them grows with time and tends to infinity. The huge difference of the field values between these two areas makes the field gradient at kinks and anti-kinks very large and in fact can be semi-analytically shown to lead to infinity in finite time [8, 7]. The existence of this kind of singularity prevents straightforward numerical integration of the space-time dependent field equation [9, 10].

In between the kinks and anti-kinks, the field gradient $\partial_i T$ does not blow up at late time. However, it has been argued that the second order spatial derivative can reach infinity in finite time, which leads to the forming of caustics [9]. This was argued to represent the crossing of streams of non-interacting tachyon matter.

The potential application of the tachyon condensation in the inflation scenario has been investigated, regardless of the various problems [11, 12, 13, 14, 15, 16]. In the tachyon inflation model, agreement with the observational data can be achieved [17]. A complex tachyon field can produce cosmic strings after inflation [18, 19, 20]. The appearance of the pressureless tachyon matter at late stage of the condensation [21, 3] is also a feature of this model. The fluctuations of the tachyon matter in both the free and the expanding cosmology background [22, 14, 16, 4, 17] have been studied, and shown to increase linearly with time, just like ordinary pressureless matter.

In this paper, we revisit tachyon condensation in order to answer two questions: are caustics generic as the work of [9] seems to imply, and do the modifications of the action proposed in [5] help to tame the singular gradients at kinks in a time-dependent situation? The ultimate aim was to try to tame the numerical instabilities of the system and to try to follow the condensation process to late time.

We will study the field equation derived from the DBI action, focusing on kinks and the extrema between kinks, and solve the perturbation equations around a homogeneous condensing field. We shall show that caustics are not generic, that

perturbations tend to “freeze”, and that the equation of state parameter of the tachyon field is generically non-zero, i.e., that tachyon matter is not quite pressureless. However, the equations are unstable, and eventually lead to a singularity.

One can ask if the instability is an artifact of the DBI effective action. To give a partial answer, we also study the boundary string field theory (BSFT) effective action [23, 24], showing that this also has a classical instability as the vacuum is approached.

Finally, we show that a modification of the action proposed by [5] to regulate the gradient at a static kink does prevent the gradient of the field reaching infinity at the kinks in the time-dependent case, but does not cure the instability of the equations between kinks. Hence, not only is numerical simulation still problematic, but the Dirac-Born-Infeld effective action itself is breaking down.

The paper is constructed as follows. In Sec. 2, we give the equation of motion and its solutions in simple cases. In Sec. 3, we present the 1 + 1 dimensional solutions near kinks and near extrema respectively. In Sec. 4 and Sec. 5, we discuss the dynamics approaching the vacuum respectively in the DBI and the BSFT effective theories. Based on the results, the features of the tachyon matter towards the end of the condensation are investigated in Sec. 6. In Sec. 7, we discuss the generalised DBI action.

2 Equation of motion

From the DBI action (1), we can write down the equation of motion:

$$\left(\square T - \frac{V'}{V}\right)(1+y) = \frac{1}{2}\partial^\mu T \partial_\mu(1+y), \quad (2)$$

where $\square = \eta_{\mu\nu}\partial^\mu\partial^\nu$. An equivalent expression to the equation of motion is

$$\dot{\pi} = f \left\{ 2\pi\nabla_i\pi\nabla^iT + (1+y)\nabla^2T - \nabla_iT\nabla_jT\nabla^i\nabla^jT - \frac{V'}{V}(1+y) \right\}, \quad (3)$$

where $\pi = \dot{T}$, $f = 1/(1 + \nabla_iT\nabla^iT)$, $\nabla^2 = \partial_i\partial^i$ and $i, j = 1, \dots, p$. $V(T)$ is the runaway tachyon potential and its field derivative is $V' = dV(T)/dT$. A suitable choice of potential, derived from the boundary conformal field theory on the worldsheet [25, 26], is

$$V = \frac{V_m}{\cosh(\beta T)}, \quad (4)$$

where the constant $\beta = 1$ for the bosonic string and $\beta = 1/\sqrt{2}$ for superstring.

The energy-momentum tensor is:

$$T_{\mu\nu} = V(T) \left[\frac{\partial_\mu T \partial_\nu T}{\sqrt{1 + \partial T \cdot \partial T}} - \eta_{\mu\nu} \sqrt{1 + \partial T \cdot \partial T} \right]. \quad (5)$$

2.1 The static case

For the 1-dimensional static case, the solution to the field equation is most easily found by noting that conservation of energy-momentum requires that the pressure is constant:

$$T_{11} = \frac{-V}{\sqrt{1+T'^2}} = -V_0, \quad (6)$$

where $V_0 = V(T_0)$ is the minimum potential when the maximum field T_0 is achieved at $x = x_0$. The maximum field satisfies the condition $T'|_{T=T_0} = 0$.

For the inverse hyperbolic potential (4), the equation is solvable:

$$T(x) = \frac{1}{\beta} \sinh^{-1} \left[\sqrt{\frac{1}{r^2} - 1} \sin(\beta \Delta x) \right], \quad (7)$$

where $r = V_0/V_m$ and $\Delta x = x - x_m$. It represents an array of solitonic kinks and anti-kinks. Its gradient is:

$$T' = \pm \sqrt{\frac{1-r^2}{r^2 + \tan^2(\beta \Delta x)}}. \quad (8)$$

For fixed V_m , T' tends to infinity at kinks and anti-kinks, where $\Delta x = n\pi/\beta$, as $V_0 \rightarrow 0$, which is consistent with the slow motion analysis on the moduli space of [7].

2.2 The homogeneous case

In this case, the energy density is conserved and constant:

$$T_{00} = \frac{V}{\sqrt{1-\pi^2}} = E, \quad (9)$$

which restricts $|\pi| \leq 1$.

For the potential (4), the time dependent solution is:

$$T(t) = \frac{1}{\beta} \sinh^{-1} \left[\sqrt{1 - \frac{1}{l^2}} \sinh(\beta t) \right], \quad (10)$$

and its time derivative is:

$$\pi = \pm \sqrt{\frac{l^2 - 1}{l^2 - \tanh^2(\beta t)}}, \quad (11)$$

where $l = E/V_m$ with $E > V_m$. Specially, $T = 0$, $|\pi| = \sqrt{1 - 1/l^2}$ at the beginning $t = 0$ and $|T| \rightarrow \infty$, $|\pi| \rightarrow 1$ as $t \rightarrow \infty$.

3 Solutions near kinks and extrema

In this section, we study the behaviour of solutions near stationary kinks and extrema, in order to gain insight into the singular dynamics, and to make contact with previous work [9, 8].

3.1 Around kinks

Following [8], we expand the field around a stationary kink or anti-kink located at $x = x_m$:

$$T(t, x) = a(t)\Delta x + \frac{1}{6}c(t)\Delta x^3 + \frac{1}{120}e(t)\Delta x^5 + \dots, \quad (12)$$

where $\Delta x = x - x_m$.

For the potential (44), $V'/V = -\beta^2 T$. For the potential (4), $V'/V \simeq -\beta^2 T$ when $|T|$ is small. We use this relation and the expansion (12) in the field equation around kinks and anti-kinks, where $|T|$ is small. The comparison of coefficients gives the equation:

$$\ddot{a} = \beta^2 a + \frac{2a\dot{a}^2 + c}{1 + a^2}. \quad (13)$$

We are more interested in the solution at late time when $a(t)$ becomes large. If we can neglect the contribution from $c(t)$,

$$\ddot{a} = \beta^2 a^2 + 2\dot{a}^2. \quad (14)$$

To solve the equation, we set $a = 1/z$, giving

$$\ddot{z} + \beta^2 z = 0, \quad (15)$$

with solution

$$z = z_1 \cos(\beta t) + z_2 \sin(\beta t). \quad (16)$$

By a suitable choice of the time coordinate, the solution of a can be written

$$a(t) = \frac{a_0}{\cos(\beta t)}, \quad (17)$$

where a_0 is constant. If we set $t_* = \pi/(2\beta)$, we approximately have: $a \sim 1/(t_* - t)$, which is consistent with the result of [8]. $a(t)$ grows to infinity in a finite time.

More precisely, we now also consider the evolution of the coefficient $c(t)$. With the same approximation of a being large, we can obtain the equation:

$$a^2 \ddot{c} = 8a\dot{a}\dot{c} + (7\beta^2 a^2 - 6a\ddot{a})c - 6\beta^2 a\dot{a}^2 + e. \quad (18)$$

Combining with Eq. (14) and neglecting $e(t)$, we find

$$c(t) = -\beta^2 a = -\frac{\beta^2 a_0}{\cos(\beta t)}. \quad (19)$$

Therefore, the solution near the kinks and anti-kinks can be expressed as:

$$T(t, x) = a(t) \left[\Delta x - \frac{1}{6} \beta^2 \Delta x^3 + \dots \right] \simeq \frac{a_0 \sin(\beta \Delta x)}{\beta \cos(\beta t)}. \quad (20)$$

This has the following properties at $x = x_m$: $T = 0$, $\pi = 0$, $T'(t \rightarrow \infty) \rightarrow \infty$, $\dot{\pi} = 0$ and $T'' = 0$, which are consistent with the discussion in Sec. 2.

3.2 Around extrema

The field around a stationary peak or trough at $x = x_0$ satisfies the condition $T'|_{x=x_0} = 0$. The expansion around x_0 is written:

$$T(t, x) = T_0(t) + \frac{1}{2} b(t) \Delta x^2 + \frac{1}{24} d(t) \Delta x^4 + \dots, \quad (21)$$

with $\Delta x = x - x_0$. For convenience, we only consider the behaviour around the field extrema whose values are positive $T_0(t) > 0$.

For the potential (4), $V'/V \simeq -\beta$ when T is positive. Inserting the expansion form in the field equation (3), we get:

$$\dot{\pi}_0 = (\beta + b)(1 - \pi_0^2). \quad (22)$$

with $\pi_0 = \dot{T}_0$. The final value of π_0 is decided by the relation between $b(t)$ and β . Here we only consider two special cases. When $b = -\beta$, π_0 is constant and it corresponds to the static case. This is consistent to the static analytical solution (7), which has $T'' = -\beta$ at peaks. Secondly, if $|b| \ll \beta$, there is an explicit solution for π_0

$$\pi_0 = \tanh(\beta t). \quad (23)$$

The solution satisfies $\pi_0 \in [0, 1]$.

The equation for the coefficient $b(t)$ is:

$$\ddot{b} = 2\beta b^2 - 2(\beta - b)\pi_0 \dot{b}. \quad (24)$$

Since we are considering the peaks on the positive field side $T_0 > 0$, π_0 should be positive and tends to 1. Making use of the approximation $\pi_0 \simeq 1$ for late time, Eq. (24) can be rewritten as:

$$\partial_t(\dot{b} - b^2) = -2\beta(\dot{b} - b^2). \quad (25)$$

Hence,

$$\dot{b} = b^2 + C_1 \exp(-2\beta t), \quad (26)$$

where $C_1 = \dot{b}_0 - b_0^2$ is a constant, with $b_0 = b(t=0)$ and $\dot{b}_0 = (db/dt)|_{t=0}$. We have made numerical solutions of (26). The distribution of the final values as a function of b_0 and \dot{b}_0 is presented in Fig. 1. From these results, we see that a peak ($b_0 < 0$) is most likely to flatten with time, but a trough ($b_0 > 1$) can deepen and become singular, and will always do so when \dot{b}_0 is positive. There is a sign of the development of a caustic.

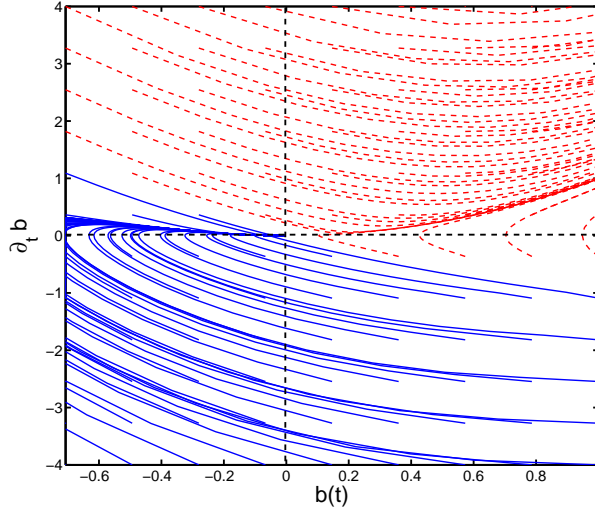


Figure 1: The time evolving curves of $\dot{b}(t)$ vs $b(t)$ with different initial values (b_0, \dot{b}_0) in regions where $b \geq -\beta$. The blue, solid lines indicate that $b(t) \rightarrow 0$ at large t and the red, dashed lines indicate that $b(t)$ tends to infinity.

3.3 Caustics around peaks?

In terms of the relations in Eq. (23) and (26), we can estimate the quantity $1 + y$ at late time as:

$$1 - \pi_0^2 - (\dot{b} - b^2)\Delta x^2 = (A - C_1\Delta x^2)e^{-2\beta t} \rightarrow 0, \quad (27)$$

which is also a result from the numerical simulations [9].

Based on this relation, the authors of [9] argue that there should be caustics forming around the peaks or troughs. They rewrite the relation (27) as a Hamilton-Jacobi equation:

$$\dot{S}^2 - S'^2 = 1, \quad (28)$$

with the approximation $S \simeq T$ and develop a series of characteristic equations for the Hamilton-Jacobi equation (28) to give

$$S''(t, x) = \frac{S''(0, x)}{1 - \frac{S''(0, x)}{(1 + S'^2(0, x))^{3/2}} t}. \quad (29)$$

Thus S'' blows up in a finite time $t = (1 + S'^2(0, x))^{3/2} / S''(0, x)$, which is interpreted as the appearance of caustics or regions where the tachyon field becomes multivalued. But in our analysis, $T'' = b(t)$ is more likely to tend to zero in the end though the possibility of $T'' \rightarrow \infty$ is not excluded. We do not use the assumption in Eq. (28).

We perform a careful analysis of the field equations in the next section which shows that the tachyon field does not quite obey Eq. (28), and that this difference is crucial.

4 Perturbations

In this section, we will consider the evolution of perturbations around a condensing homogeneous tachyon field in an arbitrary dimensional Dp -brane. This will also approximately describes the evolution of the field between well-separated kinks and anti-kinks. A general form is:

$$T(t, x^i) = T_0(t) + \tau(t, x^i), \quad (30)$$

where $\tau(t, x^i)$ is the small perturbation along all spatial directions along the Dp -brane x^i with $i = 1, \dots, p$.

A trivial case is: $T_0(t) = 0$. Around $T_0(t) = 0$, $-V'/V \simeq \beta^2\tau$ for both potentials (4) and (44). Inserting $T(t, x^i) = \tau(t, x^i)$ in the field equation (3), we can get the perturbation equation:

$$\nabla^2\tau - \ddot{\tau} + \beta^2\tau = 0, \quad (31)$$

as expected for a tachyon field with mass squared $-\beta^2$.

4.1 Perturbations around a condensing field

Plugging the ansatz (30) in the field equation with the hyperbolic potential (4), we have the zeroth and the linear order equation of τ

$$[\dot{\pi}_0 - \beta(1 - \pi_0^2)] + [\ddot{\tau} + 2\beta\pi_0\dot{\tau} - (1 - \pi_0^2)\nabla^2\tau] = 0. \quad (32)$$

First, we solve the zeroth order equation covered in the first square bracket and get the solution $\pi_0 = \tanh(\beta t)$, as given in Eq. (23).

The solution of τ in the second square bracket is separate, and writing $\tau(t, x) = f(t)g(x)$, and we find:

$$\begin{cases} \nabla^2 g + k^2 g = 0, \\ \ddot{f} + 2\beta \tanh(\beta t) \dot{f} + k^2 \operatorname{sech}^2(\beta t) f = 0, \end{cases} \quad (33)$$

where $k^2 = k_i k^i$ and k^i are arbitrary constants.

By making the reparameterisation

$$\rho = \frac{1}{1 + e^{-2\beta t}}, \quad (\frac{1}{2} \leq \rho \leq 1), \quad (34)$$

we can rewrite the second equation in Eq. (33) as

$$\rho(1 - \rho) \frac{d^2 f}{d\rho^2} + \kappa^2 f = 0. \quad (35)$$

where $\kappa^2 = \kappa_i \kappa^i$ and $\kappa_i = k_i/\beta$. It is a typical hypergeometric differential equation. The equation has two linearly independent solutions, the simpler one of which is given as [27]

$$f(t) = \rho(t) {}_2F_1 \left(\frac{1 - \sqrt{1 + 4\kappa^2}}{2}, \frac{1 + \sqrt{1 + 4\kappa^2}}{2}; 2; \rho(t) \right), \quad (36)$$

where ${}_2F_1$ is the hypergeometric function.

We will focus on the late time behaviour of τ when π_0 is closed to 1. In this situation, the second equation in Eq. (33) becomes $\ddot{f} + 2\beta\dot{f} + 4k^2 \exp(-2\beta t)f = 0$. With the reparameterization $\eta = \exp(-2\beta t)$, we have:

$$\eta \frac{d^2 f}{d\eta^2} + \kappa^2 f = 0. \quad (37)$$

The equation is a Bessel style differential equation [28]. Its solution is given as a combination of two Bessel functions. The whole solution at late time can be expressed as:

$$\tau(t, x^i) = \int \frac{d^p k}{(2\pi)^p} \left[\tau_1(k_i) h^{(1)}(t, k) e^{ik_i x^i} + \tau_2(k_i) h^{(2)}(t, k) e^{-ik_i x^i} \right], \quad (38)$$

where $\tau_1(k_i)$, $\tau_2(k_i)$ are constant parameters corresponding to the mode k_i and

$$h^{(1,2)}(t, k) = e^{-\beta t} H_1^{(1,2)}(2\kappa e^{-\beta t}). \quad (39)$$

$H_1^{(1,2)}(s)$ are the Hankel function, which are the linear combinations of the Bessel function of the first kind $J_1(s)$ and the second kind $Y_1(s)$: $H_1^{(1)}(s) = J_1(s) + iY_1(s)$ and $H_1^{(2)}(s) = J_1(s) - iY_1(s)$. They satisfy $H_1^{(1)}(s) = H_1^{(2)}(s)^*$. In order to get $\tau = \tau^*$, $\tau_1(k_i) = \tau_2(k_i)^*$. Then we can set $\tau_1(k_i) = \tau_0(k_i) e^{i\delta(k_i)}$ and $\tau_2(k_i) = \tau_0(k_i) e^{-i\delta(k_i)}$.

Here, we consider the real tachyon field T . The perturbation (38) should be real as well and can be expressed as, denoting $s = 2\kappa e^{-\beta t}$:

$$\tau(t, x^i) = \int \frac{d^p k}{(2\pi)^p} \frac{s}{2\kappa} \tau_0(k_i) \left[J_1(s) \cos(k_i x^i + \delta(k_i)) - Y_1(s) \sin(k_i x^i + \delta(k_i)) \right]. \quad (40)$$

For small parameters $0 < s \ll \sqrt{2}$,

$$J_1(s) \simeq \frac{s}{4}, \quad Y_1(s) \simeq -\frac{2}{\pi s}. \quad (41)$$

Thus, at late time, Eq. (40) approximately reduces to:

$$\tau \simeq \frac{\beta}{\pi} \int \frac{d^p k}{(2\pi)^p} \frac{\tau_0(k_i)}{k} \sin(k_i x^i + \delta(k_i)). \quad (42)$$

The result indicates that the perturbation corresponding to each mode k_i freezes at late time and that shorter wavelength modes are damped more than longer wavelength. It also provides evidence that caustics are not inevitable, as there is no divergence in T'' .

4.2 Comparison with the numerical simulations

We make numerical simulations of the perturbations based on the field equation in Eq. (3) for the 1 + 1 dimensional case. In all simulations, the constant $\beta = 1/\sqrt{2}$. The simulation is implemented on a spatial lattice of 128 points. The lattice spacing and the timestep are set to be respectively: $\delta x = 0.125$ and $\delta t = 6 \times 10^{-4}$. We use the symmetric difference for the first order field derivatives and a 3-point stencil for the second order field derivatives. We adopt the second order Runge-Kutta method for the time update.

To get the perturbation, we first need to produce two sets of simulation data with two different initial conditions respectively: $T(t = 0, x) = D$ and $T(t = 0, x) = D + 0.01 \sin(kx)$, where D is the field value at $t = 0$: $D = T_0(t = 0)$. The difference between them gives the 1 + 1 dimensional evolution surface of $\tau(t, x, k)$. In Fig. 2, we only present the amplitude curves of the perturbations with different k , which are compared with the corresponding plots of the hypergeometric solution given in Eq. (36). We can see that their late time behaviour fits well qualitatively, but in the initial stages there is a big difference. The reason should be that we only plot one of the two linearly independent hypergeometric solutions. The real solution should be a combination of the two, which could in principle be calculated if required.

4.3 Instability near the vacuum

We have seen that $T \rightarrow \infty$ and $V \rightarrow 0$ as $t \rightarrow \infty$ at extrema, which is the open string vacuum where no open string excitation states should exist as conjectured by Sen [29]. Let us look at the behaviour near this vacuum.

For large T , we can assume that $\pi \rightarrow 1$, $\dot{\pi} \rightarrow 0$ and $V'/V \simeq -\beta$. Then the equation of motion (2) becomes

$$\frac{\partial}{\partial t}(1 + y) \simeq -2(\nabla^2 T + \beta)(1 + y) + 2\nabla_i T \nabla_j T \nabla_i \nabla_j T - \pi \frac{\partial}{\partial t}(\nabla^2 T). \quad (43)$$

Consider the small perturbations around a linearly increasing field $T_0 \gg 1$. We have the perturbation of the form: $T(x) = T_0(t) + \tau(t, x^i)$. As we have seen,

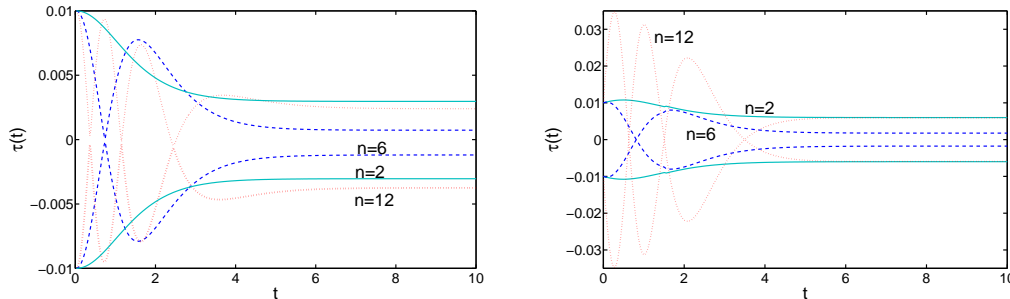


Figure 2: Left: The amplitude profiles of $\tau(t, x, k)$ around a large field $T_0(t)$ from the lattice simulations based on Eq. (3). The initial field and the initial perturbation are respectively set to be $\pi_0(t=0) = 0$, $T_0(t=0) = D = 10$ and $\tau(t=0, x) = 0.01 \sin(kx)$, with $k = 2\pi n/L$ and $L = 16$. Right: The plots of the hypergeometric solution $\tau(t) = f(t)$ given in Eq. (36).

τ freezes at later time. Thus, the last term in Eq. (43) vanishes at late time. If the last two terms are negligible, the quantity $1 + y$ will decrease exponentially with time.

To check this expectation, we have performed numerical simulations in $1 + 1$ dimensions on a spatial lattice of size 1280 sites. The spacing and the timestep are respectively: $\delta x = 0.025$ and $\delta t = 5 \times 10^{-3}$. The field on each site is chosen from a Gaussian distribution with mean 0 and standard deviation 0.1 and its rate of change is zero. We adopt a smooth random initial condition, in which the field evolves according to $\dot{T} = \nabla^2 T$ until wavelengths $\lambda_s < 2\pi\sqrt{0.4}$ are exponentially damped. The results are presented in Fig. 3, which shows that $1 + y$ really decreases with time to very small positive values exponentially.

However, in the meanwhile, there is instability emerging in a finite time which terminates the simulations. One can see singularities developing fast at $x = 27$ and also around $x = 4$. In terms of the perturbation equation (32), we note that there is an instability when π^2 exceeds 1. In Fig. 3b, we plot $1 - \pi^2$, which indeed shows that the first region to go unstable has the most negative value of $1 - \pi^2$.

This instability is generic. Eq. (43) shows that $1 + y$ will vanish, which means that $1 - \pi^2$ will go negative in some places, leading to exponential growth in the perturbations in those regions.

5 The BSFT action

The effective action derived from BSFT is given by [23, 24]: $\mathcal{L} = -V(T)F(y)$ with the potential

$$V(T) = \exp\left(-\frac{\beta^2 T^2}{2}\right), \quad (44)$$

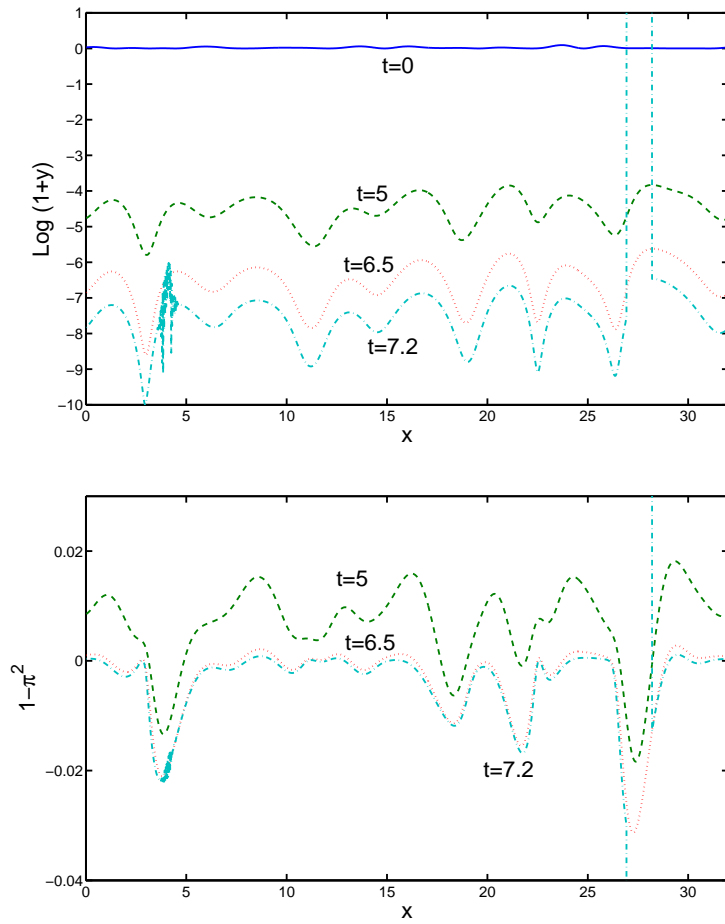


Figure 3: The plots of the quantities $\log(1 + y)$ and $1 - \pi^2$. The quantity $1 + y$ decreases with time. Dramatic instability happens where $|\pi|$ exceeds 1 the most.

and the kinetic part

$$F(y) = \frac{1}{2} \frac{4^y y \Gamma^2(y)}{\Gamma(2y)} = 2^{2y-1} y B(y), \quad (45)$$

where $y = \partial^\mu T \partial_\mu T$ as before and $B(y)$ is the beta function. It is easy to see that $F \geq 0$ when $y \geq -1/2$. The formulas of the gamma function and the beta function adopted in this section can be found in general mathematical tool books, e.g., [28].

Using $\Gamma(1+u) = u\Gamma(u)$, we can derive the recursion relation

$$B(y) = 2^{2m} \frac{(y + \frac{2m-1}{2})(y + \frac{2m-3}{2}) \cdots (y + \frac{1}{2})}{(y+m-1)(y+m-2) \cdots (y+1)y} B(y+m), \quad m = 1, 2, 3, \dots \quad (46)$$

From Stirling's approximation, $B(u) \simeq 2^{1-2u} \sqrt{\pi/u}$ for large u . For $m = 1$, we approximately have

$$F(y) = 2^{2y+1} (y + \frac{1}{2}) B(1+y) \simeq \sqrt{\pi} \sqrt{1+y}, \quad (47)$$

when $1+y \gg 1$. This is the DBI action. So the behaviour of the BSFT action (45) for large $1+y$ should be similar to that discussed in previous sections. In what follows, we will discuss the behaviour near the vacuum when y is small or negative.

5.1 Time evolution

We first explore the homogeneous approach to the vacuum. The equation of motion in this case is

$$F - 2yF' = \frac{E}{V}, \quad (48)$$

where $y = -\dot{T}^2$, $F' = \partial F / \partial y$ and E is a constant.

The condensation starts with a small velocity $|\dot{T}|$. Let us consider the case when $\dot{T} = 0$. With the relation of the gamma function $\Gamma(2u) = 2^{2u-1} \Gamma(u) \Gamma(u + 1/2) / \sqrt{\pi}$, we can rewrite the kinetic part $F(y)$ as

$$F(y) = \sqrt{\pi} \frac{\Gamma(y+1)}{\Gamma(y+\frac{1}{2})}. \quad (49)$$

Thus, $F(0) = 1$ since $\Gamma(1/2) = \sqrt{\pi}$. This gives $V(T) = E$ at $\dot{T} = 0$ in terms of the equation of motion.

Now we need to find where the tachyon potential gets the minimum value $V(T) = 0$, which corresponds to the vacuum. Since $y = -\dot{T}^2 \leq 0$ in the homogeneous case, we can change the action to the form by using $\Gamma(1-u)\Gamma(u) = \pi / \sin(\pi u)$

$$F(y) = -2^{2y+1} \pi \cot(\pi y) \frac{1}{B(-y)} \simeq -\sqrt{\pi} \cot(\pi y) \sqrt{-y}. \quad (50)$$

Then the homogeneous equation of motion (48) becomes

$$\frac{2(-\pi y)^{\frac{3}{2}}}{\sin^2(\pi y)} \simeq \frac{E}{V}. \quad (51)$$

It is easily seen that $V = 0$ at $y = -n$, where $n = 1, 2, 3, \dots$. The behaviour in taking the limit $\dot{T}^2 \rightarrow n$ is,

$$V(T) \sim \frac{E}{2} \sqrt{\frac{\pi}{n^3}} (\dot{T}^2 - n)^2. \quad (52)$$

The equation implies that the tachyon potential vanishes for either $\dot{T}^2 \rightarrow n$ or $n \rightarrow \infty$. We will assume that only the first pole ($y = -1$) in Eq. (51) is relevant, as the condensation starts with $y \simeq 0$.

5.2 Dynamics near the vacuum

The full equation of motion for a general $F(y)$ is

$$\left(2 \frac{F''}{F'} \partial_\mu T \partial_\nu T + \eta_{\mu\nu} \right) \partial^\mu \partial^\nu T + \frac{V'}{V} \left(y - \frac{1}{2} \frac{F}{F'} \right) = 0. \quad (53)$$

Note that $V' = \partial V / \partial T$, $F' = \partial F / \partial y$ and $F'' = \partial^2 F / \partial y^2$.

We now consider the dynamics approaching the vacuum when $y \rightarrow -1$ from above. Using Eq. (46), the BSFT action can be expressed as

$$F(y) \simeq \frac{(y + \frac{2m-1}{2})(y + \frac{2m-3}{2}) \cdots (y + \frac{1}{2})}{(y + m - 1)(y + m - 2) \cdots (y + 1)} \sqrt{\frac{\pi}{y + m}}, \quad (54)$$

and we will find it useful to take $m \gg -y$.

Since $F/F' = 1/(\ln F)'$ and $F''/F' = (\ln F)''/(\ln F)' + (\ln F)'$, we only need to know $(\ln F)'$ and $(\ln F)''$ for deriving the equation of motion. In the limit $y \rightarrow -1$, we approximately have for any $m \geq 2$

$$(\ln F)' \sim -\frac{1}{1+y}, \quad (\ln F)'' \sim \frac{1}{(1+y)^2}. \quad (55)$$

The corresponding expressions for the DBI action are $(\ln F)' = 1/[2(1+y)]$ and $(\ln F)'' = -1/[2(1+y)^2]$. Inserting them in the equation of motion, we have

$$\left(\square T - \frac{V'}{V} \right) (1+y) \simeq 2\partial^\mu T \partial_\mu (1+y), \quad (56)$$

So it is very similar to Eq. (2) for the DBI action. The only difference is a change of the coefficient on the right hand side. Therefore, there should be similar consequences for the dynamics approaching the vacuum from the BSFT action to those from the DBI action. That is, the perturbations freeze and instability emerges towards the end of the condensation.

6 Tachyon matter

Reverting to the DBI action, the energy density and the pressure are given in flat spacetime by Eq. (5):

$$\rho = T_{00} = \frac{1 + (\nabla T)^2}{\sqrt{1 + y}} V(T), \quad (57)$$

$$p_i = T_{ii} = -V(T) \frac{1 + y - (\partial_i T)^2}{\sqrt{1 + y}} = q + \frac{(\partial_i T)^2}{1 + (\nabla T)^2} \rho, \quad (58)$$

where there is no sum on i and $q = \mathcal{L} = -V(T)\sqrt{1 + y}$, and so

$$w_i = \frac{p_i}{\rho} = -\frac{1 + y}{1 + (\nabla T)^2} + \frac{(\partial_i T)^2}{1 + (\nabla T)^2}. \quad (59)$$

From the above formulas, it is easy to see that the system at the beginning of the tachyon condensation has positive energy density and negative pressure everywhere: $p_i = -\rho = -V_m$, the characteristic of the interior of a brane. After the condensation starts, the behavior in different areas becomes different.

Consider the case that the decay of the Dp -brane happens only in the x^1 direction to produce a $D(p - 1)$ -brane. Then the decay process can be described by a kink-anti-kink tachyon solution along the x^1 direction.

First, we consider the appearance of a $D(p - 1)$ -brane, which we locally choose to be orthogonal to the x^1 -direction. Since $\pi = 0$ and $|\partial_1 T| \rightarrow \infty$ towards the end of the decay at kinks, the energy density near the kinks $\rho_K \rightarrow \infty$. If the approximate solution found in Sec. 3.1 is to be believed, this divergence happens in finite time, in accordance with the analysis in the string field theory [30, 31]. The pressure components in all p spatial directions are respectively: $p_{jK} = q$ ($2 \leq j \leq p$) and

$$p_{1K} = p_{jK} + \frac{(\partial_1 T)^2}{1 + (\partial_1 T)^2} \rho_K. \quad (60)$$

Therefore, $p_{jK} \simeq -\rho_K$ and $p_{1K} \simeq p_{jK} + \rho_K$ near the end of the condensation. And so $p_{jK} \rightarrow -\infty$ and $p_{1K} \rightarrow 0$ as $t \rightarrow \infty$, which further give $w_{jK} \rightarrow -1$ and $w_{1K} \rightarrow 0$. This is consistent with the appearance of a $D(p - 1)$ -brane in a vacuum.

Second, we consider the approach to vacuum of a homogeneous field with small perturbations. The energy density ρ_V and the pressure p_{iV} near the vacuum can be analysed using the results of the previous section. The final values of ρ_V and p_{iV} at the end of the condensation are not obviously determined because the two quantities $V(T)$ and $1 + y$ both tend to zero as $t \rightarrow \infty$. They can be estimated in terms of Eq. (43). When $\nabla_i \tau \simeq 0$, Eq. (43) reduces to Eq. (22) with the last two terms vanishing. If we neglect the last two terms of Eq. (43) the quantity $1 + y$ can be formally expressed as: $1 + y \propto e^{-2(\nabla^2 T + \beta)t}$. For large field, π is close to 1, and hence we can write $T(t) = D + t + \mathcal{O}(e^{-2\beta t})$, where $D \gg 1$ is a constant.

For the inverse hyperbolic potential (4), $V(T) \simeq 2V_m \exp[-\beta(D+t)]$. Thus the energy density near the vacuum is

$$\rho_V \simeq 2V_m e^{-\beta D} e^{(\nabla^2 T)t}. \quad (61)$$

There are two situations for the final values of ρ_V as $t \rightarrow \infty$: (i) For peaks ($\nabla^2 T < 0$), ρ_V drops to zero; (ii) For troughs ($\nabla^2 T > 0$), ρ_V grows to infinity in the end. The linear analysis is similar to the analysis of the behaviour of a stationary extremum in Section 3, in that a singularity emerges near a trough ($\nabla^2 T = b \rightarrow \infty$). However, in the linear analysis, this singularity is in the energy density only, and not in $\nabla^2 T$ itself, and takes an infinite time to appear. Hence, in the linear approximation, caustics do not form in finite time.

It is interesting to note that the tachyon fluid is not quite pressureless in general. Indeed, from Eq. (58), noting that $q \rightarrow 0$ near the vacuum as $t \rightarrow \infty$, we find ρ_V : $p_{iV} \sim \rho_V (\partial_i T)^2 / [1 + (\nabla T)^2]$. Given that T ‘‘freezes’’, we see that the small fluctuations give rise to a small pressure. The equation of state parameter w_{iV} is non-zero.

7 The generalised DBI action

The problem with the divergence in the gradient of the field near kinks has been recognised for some time [9, 8, 10], and regularisations of the action proposed [5, 32] with respect to this problem, which have the important property that their static kinks have finite field gradients as the minimum potential $V_0 \rightarrow 0$. In what follows, we will consider the modified action given in [5] in the 1 + 1 dimensions:

$$\mathcal{L} = -V(T)(1+y)^{\frac{1}{2}(1+\epsilon)}. \quad (62)$$

where ϵ is a small positive value. The equation of motion from it is:

$$\begin{aligned} \ddot{\pi} = & f \left\{ 2(1-\epsilon^2)\pi \nabla_i T \nabla^i \pi - \frac{V'}{V}(1+y)(1-\epsilon y) \right. \\ & \left. + (1+\epsilon)[(1+y)\nabla^2 T - (1-\epsilon)\nabla_i T \nabla_j T \nabla^i \nabla^j T] \right\}, \end{aligned} \quad (63)$$

where $f = 1/[(1+\epsilon)(1+\nabla_i T \nabla^i T - \epsilon\pi^2)]$.

First, We consider the field expansion around the kinks and antikinks in the case with the hyperbolic potential (4). Doing the field expansion like (12), we get the equation of $a(t)$:

$$\ddot{a} = \frac{\beta^2 a}{1+\epsilon} - \frac{\epsilon \beta^2 a^3}{1+\epsilon} + \frac{(1-\epsilon)(2a\dot{a}^2 + c)}{1+a^2} + \epsilon c. \quad (64)$$

So when a grows large and satisfies $1 \ll a \ll 1/\sqrt{\epsilon}$, we have a similar solution to Eq. (17). When $a \gg 1/\sqrt{\epsilon}$, the a^3 term becomes important and a begins to execute damped oscillations. a settles to $a = 1/\sqrt{\epsilon}$.

To show this point clearly, we can transform Eq. (64) into a soluble form, assuming $1 + a^2 \simeq a^2$, and neglecting c . When $\epsilon \neq 1/2$, we set $a = z^{-1/(1-2\epsilon)}$ and then have:

$$\ddot{z} + \frac{\partial U(z)}{\partial z} = 0, \quad (65)$$

where $U(z)$ is:

$$U(z) = \frac{\left(\frac{1}{2} - \epsilon\right) \beta^2 z^2}{(1 + \epsilon)} \left[1 + \left(\frac{1}{2} - \epsilon\right) z^{-\frac{2}{1-2\epsilon}} \right], \quad (66)$$

For $\epsilon > 0$, the minimum value of $U(z)$ happens at $z = \epsilon^{(1/2-\epsilon)}$ or

$$a = \frac{1}{\sqrt{\epsilon}}. \quad (67)$$

This value should be the final field gradient $T' \simeq a$ as $t \rightarrow \infty$. When $\epsilon = 1/2$, we can set $a = e^z$ and get the same equation as in (65) but with a different potential $U(z)$:

$$U(z) = \frac{\beta^2}{6} (e^{2z} - 4z). \quad (68)$$

The position according for the minimum potential $U(z)$ is $z = \ln \sqrt{2}$ or $a = \sqrt{2}$, which is consistent to the above result of $\epsilon \neq 1/2$.

For the expansion around extrema, we get:

$$\dot{\pi}_0 = \left[\frac{1 + \epsilon \pi_0^2}{1 + \epsilon} \beta + b \right] \frac{1 - \pi_0^2}{1 - \epsilon \pi_0^2}. \quad (69)$$

When $\epsilon < 1$, $1 - \epsilon \pi_0^2$ is always positive if $|\pi_0| \leq 1$. Similar to the analysis for the DBI action with $\epsilon = 0$, $|\pi_0|$ still goes to 1 here at the end of the condensation.

With the approximation $\pi_0 \simeq 1$ for positive T_0 , the equation for $b(t)$ can be expressed as:

$$(1 - \epsilon) \partial_t (\dot{b} - b^2) = -2(\beta - \epsilon b)(\dot{b} - b^2). \quad (70)$$

For $\epsilon < 1$, it can be shown both analytically and numerically that there are still two possible final values for $b(t)$ at $t \rightarrow \infty$. When b tends to zero, we can write the solution similar to (25). So it can evolve to zero at $t \rightarrow \infty$. When $b(t \rightarrow \infty) \rightarrow \infty$, b grows to infinity more quickly than the case with $\epsilon = 0$. Thus caustics are possible to form for the modified DBI action.

To discuss the perturbations, we also use the ansatz: $T(t, x^i) = T_0(t) + \tau(t, x^i)$. For the case $T_0(t) = 0$, the perturbation equation becomes:

$$\nabla^2 \tau - \ddot{\tau} + \frac{\beta^2}{1 + \epsilon} \tau = 0. \quad (71)$$

The modification of the DBI action only changes the mass squared of the tachyon profile solution. For large $T_0(t)$, the perturbation equation is approximately:

$$\left[\dot{\pi}_0 - \beta \frac{1 + \epsilon \pi_0^2}{1 + \epsilon} \frac{1 - \pi_0^2}{1 - \epsilon \pi_0^2} \right] + \left[\ddot{\tau} + \frac{2\beta \pi_0 (1 - \epsilon + 2\epsilon \pi_0^2)}{(1 + \epsilon)(1 - \epsilon \pi_0^2)} \dot{\tau} - \frac{1 - \pi_0^2}{1 - \epsilon \pi_0^2} \nabla^2 \tau \right] = 0. \quad (72)$$

The perturbation can still be split into two independent parts: $\tau(t, x) = f(t)g(x)$. When $\epsilon < 1$ and π_0 approaches 1, behaviour of the perturbation described by the equation should be similar to that of (32): instabilities will always appear in regions where $1 - \pi_0^2$ is negative.

Hence, although this modified effective action solves the problem of diverging gradients near kinks, it still has unstable solutions and breaks down as the vacuum is approached.

8 Conclusions

We have investigated the inhomogeneous tachyon condensation process, focusing on the solutions near kinks (where $T = 0$) and also in regions where the field is approximately uniform.

We obtained an approximate space-time dependent solution near the kinks and anti-kinks, verifying that the spatial derivative of the field T' tends to infinity in a finite time. We show that this singularity can be avoided by modifying the effective action in $1 + 1$ dimensions, which is consistent with the result obtained in the static case by [5, 32].

We then studied inhomogeneous tachyon condensation in the absence of kinks. In (27), an analysis assuming that the tachyon field obeyed a Hamilton-Jacobi equation $\dot{T}^2 + \nabla^2 T^2 = 1$ appeared to show that the production of caustics in finite time was unavoidable. In dropping this assumption, we find that the appearance of caustics is possible near stationary extrema but is not generic, and only happens at $t \rightarrow \infty$. Indeed, linear perturbations “freeze” and do not form caustics. However, the energy density ρ_V does diverge as $t \rightarrow \infty$ near troughs (extrema with $\nabla^2 T > 0$). The pressure of tachyon matter is small, but the equation of state parameter w does not generically vanish. These results call into question a simple model of tachyon dynamics in terms of free-streaming tachyon matter.

We also found that there is an instability in the classical field equations near extrema in both the DBI and the BSFT effective theories. What is more, a simple proposal for modifying the effective action [5, 32] does not cure this instability. This signals the breakdown of the simple effective action (1) for describing the dynamics of the tachyon field near the vacuum.

References

- [1] M. R. Garousi, *Tachyon couplings on non-bps d-branes and dirac-born-infeld action*, *Nucl. Phys.* **B584** (2000) 284–299, [[hep-th/0003122](#)].
- [2] E. A. Bergshoeff, M. de Roo, T. C. de Wit, E. Eyras, and S. Panda, *T-duality and actions for non-bps d-branes*, *JHEP* **05** (2000) 009, [[hep-th/0003221](#)].
- [3] A. Sen, *Field theory of tachyon matter*, *Mod. Phys. Lett.* **A17** (2002) 1797–1804, [[hep-th/0204143](#)].
- [4] K. Hashimoto and N. Sakai, *Brane - antibrane as a defect of tachyon condensation*, *JHEP* **12** (2002) 064, [[hep-th/0209232](#)].
- [5] P. Brax, J. Mourad, and D. A. Steer, *Tachyon kinks on non bps d-branes*, *Phys. Lett.* **B575** (2003) 115–125, [[hep-th/0304197](#)].
- [6] C.-j. Kim, Y.-b. Kim, and C. O. Lee, *Tachyon kinks*, *JHEP* **05** (2003) 020, [[hep-th/0304180](#)].
- [7] M. Hindmarsh and H. Li, *Perturbations and moduli space dynamics of tachyon kinks*, *Phys. Rev.* **D77** (2008) 066005, [[arXiv:0711.0678](#)].
- [8] J. M. Cline and H. Firouzjahi, *Real-time d-brane condensation*, *Phys. Lett.* **B564** (2003) 255–260, [[hep-th/0301101](#)].
- [9] G. N. Felder, L. Kofman, and A. Starobinsky, *Caustics in tachyon matter and other born-infeld scalars*, *JHEP* **09** (2002) 026, [[hep-th/0208019](#)].
- [10] N. Barnaby, A. Berndsen, J. M. Cline, and H. Stoica, *Overproduction of cosmic superstrings*, *JHEP* **06** (2005) 075, [[hep-th/0412095](#)].
- [11] A. Mazumdar, S. Panda, and A. Perez-Lorenzana, *Assisted inflation via tachyon condensation*, *Nucl. Phys.* **B614** (2001) 101–116, [[hep-ph/0107058](#)].
- [12] M. Fairbairn and M. H. G. Tytgat, *Inflation from a tachyon fluid?*, *Phys. Lett.* **B546** (2002) 1–7, [[hep-th/0204070](#)].
- [13] D. Choudhury, D. Ghoshal, D. P. Jatkar, and S. Panda, *On the cosmological relevance of the tachyon*, *Phys. Lett.* **B544** (2002) 231–238, [[hep-th/0204204](#)].
- [14] L. Kofman and A. Linde, *Problems with tachyon inflation*, *JHEP* **07** (2002) 004, [[hep-th/0205121](#)].

- [15] M. Sami, P. Chingangbam, and T. Qureshi, *Aspects of tachyonic inflation with exponential potential*, *Phys. Rev.* **D66** (2002) 043530, [[hep-th/0205179](#)].
- [16] G. Shiu and I. Wasserman, *Cosmological constraints on tachyon matter*, *Phys. Lett.* **B541** (2002) 6–15, [[hep-th/0205003](#)].
- [17] D. A. Steer and F. Vernizzi, *Tachyon inflation: Tests and comparison with single scalar field inflation*, *Phys. Rev.* **D70** (2004) 043527, [[hep-th/0310139](#)].
- [18] G. R. Dvali and S. H. H. Tye, *Brane inflation*, *Phys. Lett.* **B450** (1999) 72–82, [[hep-ph/9812483](#)].
- [19] S. Sarangi and S. H. H. Tye, *Cosmic string production towards the end of brane inflation*, *Phys. Lett.* **B536** (2002) 185–192, [[hep-th/0204074](#)].
- [20] D. Choudhury, D. Ghoshal, D. P. Jatkar, and S. Panda, *Hybrid inflation and brane-antibrane system*, *JCAP* **0307** (2003) 009, [[hep-th/0305104](#)].
- [21] A. Sen, *Tachyon matter*, *JHEP* **07** (2002) 065, [[hep-th/0203265](#)].
- [22] A. V. Frolov, L. Kofman, and A. A. Starobinsky, *Prospects and problems of tachyon matter cosmology*, *Phys. Lett.* **B545** (2002) 8–16, [[hep-th/0204187](#)].
- [23] D. Kutasov, M. Marino, and G. W. Moore, *Remarks on tachyon condensation in superstring field theory*, [hep-th/0010108](#).
- [24] P. Kraus and F. Larsen, *Boundary string field theory of the DD-bar system*, *Phys. Rev.* **D63** (2001) 106004, [[hep-th/0012198](#)].
- [25] D. Kutasov and V. Niarchos, *Tachyon effective actions in open string theory*, *Nucl. Phys.* **B666** (2003) 56–70, [[hep-th/0304045](#)].
- [26] M. Smedback, *On effective actions for the bosonic tachyon*, *JHEP* **11** (2003) 067, [[hep-th/0310138](#)].
- [27] A. Jeffrey and D. Zwillinger, *Table of Integrals, Series, and Products*. 2007. Academic Press.
- [28] M. Abramowitz and I. A. Stegun, *Handbook of Mathematical Functions with Formulas, Graphs, and Mathematical Tables*. Dover, New York, ninth dover printing, tenth gpo printing ed., 1965.
- [29] A. Sen, *Tachyon dynamics in open string theory*, *Int. J. Mod. Phys.* **A20** (2005) 5513–5656, [[hep-th/0410103](#)].

- [30] A. Sen, *Rolling tachyon*, *JHEP* **04** (2002) 048, [[hep-th/0203211](#)].
- [31] F. Larsen, A. Naqvi, and S. Terashima, *Rolling tachyons and decaying branes*, *JHEP* **02** (2003) 039, [[hep-th/0212248](#)].
- [32] E. J. Copeland, P. M. Saffin, and D. A. Steer, *Singular tachyon kinks from regular profiles*, *Phys. Rev.* **D68** (2003) 065013, [[hep-th/0306294](#)].